nature portfolio

Peer Review File

Nano-confined controllable crystallization in supramolecular polymeric membranes for ultra-selective desalination

Corresponding Author: Dr Shuang Zheng

Parts of this Peer Review File have been redacted as indicated to maintain the confidentiality of unpublished data.

This file contains all reviewer reports in order by version, followed by all author rebuttals in order by version.

Version 0:

Reviewer comments:

Reviewer #1

(Remarks to the Author)
In this work, the authors synthesized amphiphilic oligomers with star-shaped hydrophobic chains capped by 2-ureido-4-pyrimidinone (tetra-PCL-UPy) polar groups, aiming to achieve a precise molecular arrangement at the air/air interfaces, thus enabling the so-called “nano-confined controllable crystallization (NCC)”, for the preparation of ultrathin membranes. The authors stated that their membranes (e.g., the NCC membrane with a thickness of 6 nm) were demonstrated to have exceptional mechanical robustness and durability, a homogeneous pore size distribution, and improved fractional free volume that the makes it suitable for high performance reverse osmosis desalination, with high water permeability of 14.8 LMH/bar and a water/NaCl selectivity of over 54 bar-1 in a hydraulic pressure-driven process (10 bar) with 1000 ppm NaCl as a feed solution.
Comments:
1) The authors defined their membranes (and test conditions) as suitable for reverse osmosis water desalination. However, based on the typical pore size (0.28 nm for NCC-6) of the produced membranes (being porous....) and the operating pressure (10 bar), it should be more appropriate to consider them possibly as nanofiltration membranes. In this regard, the high rejection rate of monovalent ions (99.2%), as well as bivalent ones (99.5%), is not commented, considering the porous nature of these membranes.
2) The authors did not explain in the text the specific potential field of application of desalination for their membranes. Why Authors did not test their membranes with the typical salt concentration of sea water, while the experiments were limited to investigations on a 1000 ppm saline solution containing a single salt? This is quite far from the typical concentration of water of sea (35000 ppm), therefore limiting its field of application.
3) “The star-shaped configuration allows for more controllable crystallization”. However, this requires a more thorough discussion. What does “controllable crystallization under nano-confinement” mean?
4) “The quadruple hydrogen bonding of UPy motifs enhances the interfacial bonding with water molecules, leading to greater crystalline heterogeneity in the NCC membranes.” How do the authors prove this claim?
5) The membrane NCC-6 was defect-free based on optical microscopy images. This is not the proper characterization technique to make such affirmation.
6) “With an increase in solute concentration up to 8 mg mL−1, S slightly increased and reached its maximum value, leading to an initial increase and subsequent decrease in the spreading area of the nanofilms”. How do the authors justify this behaviour?
7) “As S value decreases, the spreading rate decreases, allowing PCL chains to assemble and crosslink via sufficient folding and orientation. This leads to stronger interactions between polymer chains, resulting in an improved membrane thickness”. This is not proven. Furthermore, how could this statement fit with the fact that there was no uniform relationship between diffusion area and crystallinity of NCC membranes?
8) “NCC-6 showed a melting temperature of approximately 44°C”. How do the Authors comment on the potential real applicability of their membranes with such a low melting temperature?
9) The authors reported that, compared to the NRC-6 membrane, the NCC-6 membrane had a narrower pore size. How is this demonstrated? What about the statistical validity of such data?
10) “The intensities of the C-C stretching band of the top side are more prominent than those of the rear side, as indicated by Raman mapping (Figure 3b), suggesting the controllable crystallization of the two sides of the NCC-6 membrane”. This is rather speculative and need further demonstration.

11) The authors explained that the Janus wetting properties and chemical heterogeneity of the two sides of the NCC membranes were due to the carbonyl groups and the orientation of the Upy motif at the water/air interface. However, this type of orientation should also occur, albeit to a lesser extent, with NRC samples. Why didn't this kind of orientation occur at all in the latter case? This should be commented.
12) On page 11, the authors stated that their membranes outperformed current state-of-the-art RO membranes. However, they forget to specify under which test conditions the membranes were tested, especially considering the salt concentration used in their tests (1000 ppm and single salt).
13) It is possible to discuss “Long-term RO separation measurements” when RO refers to a solution diffusion transport mechanism, that is typical of dense membranes (or with interspace of polymer chains in the order of a few Angstroms). What about the transport mechanism in such membranes? (also, in connection to the observed rejection of boron).
14) The surface roughness of the NCC-6 membranes and their greater resistance to harsh conditions compared to the NRC-6 sample is unclear.
15) More importantly, the authors reported the highest permeability (14.8 L m-2 h-1 bar-1H) and water/NaCl selectivity (54 bar-1) among current state-of-the-art RO membranes. However, in addition to not specifying the test conditions (in particular the concentration and temperature of the feed), they carried out this calculation based on weight data from a system of 3 cm2 active membrane area. Using such tiny equipment means using small feed and permeate volumes, small tube diameters, and small sensors and scales to measure the increase in permeate weight. On such a small scale, the indeterminacy of a single drop of water could make a big difference, heavily influencing the calculated transmembrane flux. Why didn't the authors use larger membranes to confirm what they obtained on such a small scale? What about the scalability of the method?

Reviewer #2

(Remarks to the Author)
The manuscript demonstrates polymeric membranes formed by controllable crystallization of oligimers. The material introduced in the work shows better permeability-selectivity performance than the polyamide-based membranes widely used for desalination. The membrane also appears to be robust under pressure, tolerate some chlorine exposure, and operate after exposure to harsh pH conditions. Overall, the work is impressive and demonstrates what appears to be a feasible chemistry to improve upon long-standing polyamide membranes. My main criticisms relate to the lack of comparisons in performance to conventional polyamide membranes and difficulty understanding the transport mechanisms in this system. Comments are further expanded upon below.

The authors emphasize strong hydrogen bonding in the abstract and also discuss the void size in molecular simulations. However, the proposed rejection mechanisms in this membrane remain unclear. The authors should consider adding a clearer discussion of rejection mechanisms so that readers can better understand which compounds are likely to be rejected and which compounds will pass through these membranes.

I would assume that the presence of a crystalline region (which does not allow for water flow) would decrease the effective membrane area, since only the amorphous regions are accessible to water. Can the authors estimate the accessible/active pore area? It is surprising the permeability can be so high with some of the pore area blocked off (e.g., compared to conventional RO membranes which presumably do not have similar impermeable regions).

I did not understand why the shape of the oligomers would result in channels. Since they are end-capped with hydrogens bonds, it seems like the center of a repeating circle would be impermeable and the outside would be permeable.

Although the membranes appear to be sufficiently robust for operation under high pressure and proof-of-concept testing, they are not crosslinked. This would make them vulnerable to breakdown at high temperature (I think the authors say NCC-6 melts around 44 °C), after solvent exposure, or possibly after exposure to surfactants. The authors should comment on limitations or areas for future work in terms of membrane robustness.

During fabrication of the films, what determines thickness? Intuitively the droplet in chloroform should continue spreading to make a very thin film. Was uniform thickness observed through the sample?

Why was long-term testing conducted at only 4 bar? Is long-term pressure stability difficult for these membranes?

The boron rejection did not appear to be particularly high. Comparison to equivalent polyamide reverse osmosis membranes may be helpful for context.

I found the chlorine and pH exposure results interesting and impressive. You may include results for conventional polyamide membranes here for context. We have found these decrease to around 50% rejection after exposure to similar chlorine doses.

Page 12, last paragraph: I did not understand comparison to the NRC-6 membranes rather than other polymeric desalination membranes.

“The nanofilm adheres firmly to the substrate due to the high density of interfacial non-covalent interactions.” I was confused about what interactions were being referred to here.

Reviewer #3

(Remarks to the Author)
The authors describe a novel self-assembly strategy of designing desalination membranes using amphiphilic oligomers with the aim to overcome the traditional permeability selectivity trade off seen in state of the art membranes. The mechanism is certainly interesting and the authors have very good results in terms of separation performance (including boron rejection) and chlorine tolerance. The characterization portion of the membrane is also very strong.

1.The weak part of this paper is the general motivation - it has been reported in the literature that there is very little need to design new desalination membranes. The current state of the art RO membranes are excellent and further enhancement in flux is not required. RO membranes, however, suffer from low boron rejection rates and low chlorine tolerance - the authors could have perhaps focused more on these two attributes that trying to improve water and salt rejection coefficients beyond commercial RO membranes.

2. With the sharp size-exclusion domains in these membranes, the authors could also consider similar ion separations or solute-solute separations - these applications could be much more impactful with this type of membrane than targeting the well-established desalination membranes.

3. The authors have provided many comparison points between the NRC and NCC membranes (of varied thicknesses) - however, they do not provide any comparison between other (related) self assembly membranes using different approaches (e.g. block copolymer etc.). It is therefore not clear how the performance of these membranes compare against membranes reported in the literature.

4. The method of membrane fabrication involving the spreading of the droplets appears to be very simple ; however, it could be very sensitive to ambient conditions and if larger membrane coupons are to be made, reproducibility/repeatability could be an issue. Could the authors shed some light on how these envision large area membranes to be made using this process?

5. The authors briefly mention that a range of supports such as polyethersulfone(PES), Silicon wafer and anodic aluminum oxide(AAO) that could be used - however, results comparing these supports are missing in the manuscript as well as the supplementary information. These results could be very valuable for this paper.

Reviewer #4

(Remarks to the Author)
I co-reviewed this manuscript with one of the reviewers who provided the listed reports. This is part of the Nature Communications initiative to facilitate training in peer review and to provide appropriate recognition for Early Career Researchers who co-review manuscripts.

Version 1:

Reviewer comments:

Reviewer #1

(Remarks to the Author)
The authors provided some reasonable responses regarding several points raised during the review process, which are related to details on definitions and procedure; they also increased clarity of discussion in some parts. However, in this reviewer's opinion, this work has some basic weaknesses that were not addressed in the revised manuscript. The authors claim that their membranes “exceed the upper limit of water/NaCl selectivity observed in current state-of-the-art RO and NF membranes.” However, this comparison does not take into account the different experimental conditions under which the membrane performance was determined. They continue to consider 1000 ppm of NaCl solution as the feed at 10 bar and 25 °C for data in Fig. 4e. The aforementioned performance improvement of these membranes should be due to the "peculiar" transport mechanism across the membrane, based on continuous water channels occurring with a very narrow pore size (and small) distribution, while the high selectivity is explained by considering the solvation energy of sodium. They made some molecular dynamics simulations; however, such kind of mechanisms have not been proven in the real world. Also, about the melting temperature of 44°C for their membranes, Authors replied that “…. Operational conditions for many desalination applications …. Typically remain well below this temperature.” This reviewer is aware of this, however an optimal operating temperature suggested by a membrane manufacturer for its product is a different thing than a temperature at which the product melts ……. Finally, under the request to provide evidence on potential scalability of such membrane data, that were obtained with a module of size let’s say 3x4 cm2, Authors reported data collected with a module of 4x5 cm2 … this is not really a scaleup.

Reviewer #2

(Remarks to the Author)
The authors have sufficiently addressed my comments in the revision. I appreciate the authors adding text on the limitations of the developed membranes.

Reviewer #3

(Remarks to the Author)
The authors have addressed the comments well - I have no further comments or suggestions.

Reviewer #4

(Remarks to the Author)
I co-reviewed this manuscript with one of the reviewers who provided the listed reports. This is part of the Nature Communications initiative to facilitate training in peer review and to provide appropriate recognition for Early Career Researchers who co-review manuscripts.

Reviewer #1 (Remarks to the Author):

In this work, the authors synthesized amphiphilic oligomers with star-shaped hydrophobic chains capped by 2-ureido-4-pyrimidinone (tetra-PCL-UPy) polar groups, aiming to achieve a precise molecular arrangement at the air/air interfaces, thus enabling the so-called "nano-confined controllable crystallization (NCC)", for the preparation of ultrathin membranes. The authors stated that their membranes (e.g., the NCC membrane with a thickness of 6 nm) were demonstrated to have exceptional mechanical robustness and durability, a homogeneous pore size distribution, and improved fractional free volume that the makes it suitable for high performance reverse osmosis desalination, with high water permeability of 14.8 LMH/bar and a water/NaCl selectivity of over 54 bar-1 in a hydraulic pressure-driven process (10 bar) with 1000 ppm NaCl as a feed solution.

Response:

We appreciate the reviewer's thorough evaluation of our work on the synthesis of amphiphilic oligomers for the creation of ultrathin membranes with exceptional properties. Below, we have carefully addressed each of the detailed concerns put forth by the reviewer.

Comments:

1) The authors defined their membranes (and test conditions) as suitable for reverse osmosis water desalination. However, based on the typical pore size (0.28 nm for NCC-6) of the produced membranes (being porous....) and the operating pressure (10 bar), it should be more appropriate to consider them possibly as nanofiltration membranes. In this regard, the high rejection rate of monovalent ions (99.2%), as well as bivalent ones (99.5%), is not commented, considering the porous nature of these membranes.

Response:

We appreciate your observations regarding the classification of our membranes based on pore size and operating conditions. We acknowledge that the pore radius of 0.28 nm suggests characteristics typical of nanofiltration membranes, it is important to note that NF membranes typically exhibit lower salt rejection rates for monovalent ions (70–90%), particularly NaCl, where the separation effect is less pronounced compared to divalent salts. In our study, however, we observed high salt rejection rates of 99.2% for monovalent ions and 99.5% for divalent ions. This can be attributed to the narrowed size distribution of nanopores within our membranes.

To further evaluate the desalination performance for brackish water and seawater, we conducted additional experiments using the NCC-6 membrane with a 2000 ppm NaCl solution at 15.5 bar and a 35,000 ppm NaCl solution at 55 bar. The NCC-6 membranes demonstrated high water flux and NaCl rejection rates exceeding 99.2% (Figure R1), indicating their effectiveness for brackish water/seawater reverse osmosis desalination.

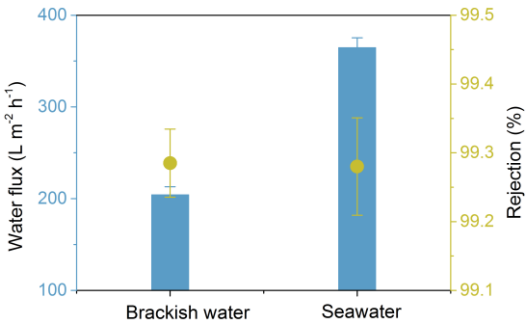

Figure R1. Water flux and rejection of the NCC-6 membrane treated with brackish water/seawater.

In summary, our membranes exhibit high water flux and rejection of monovalent ions in desalinating brackish water and seawater, primarily due to the narrowed size distribution of nanopores.

2) The authors did not explain in the text the specific potential field of application of desalination for their membranes. Why Authors did not test their membranes with the typical salt concentration of sea water, while the experiments were limited to investigations on a 1000 ppm saline solution containing a single salt? This is quite far from the typical concentration of water of sea (35000 ppm), therefore limiting its field of application.

Response:

We appreciate the reviewer's insightful comment regarding the potential applications of our membranes in desalination. We acknowledge the importance of clarifying the specific field of application for our membranes.

Our initial studies focused on a 1000 ppm saline solution primarily to isolate the effects of individual salts and to simplify the analysis of membrane performance. This approach allowed us to gain a clearer understanding of the membranes' rejection capabilities under controlled conditions.

To strengthen the relevance and applicability of our research, we have conducted additional desalination tests on NCC membranes treated with a 35000 ppm NaCl solution at 55 bar, as indicated in Figure R2. Our NCC membranes exhibited high water flux and rejection exceeding 99.2%, with the NCC-6 showing a water flux over 360 LMH.

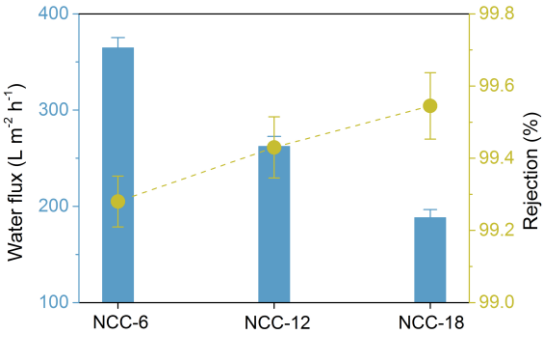

Figure R2. Water flux and rejection of NCC membranes tested with a 35000 ppm NaCl solution and 55 bar.

In addition, we have evaluated desalination performance of the NCC-6 membrane using a synthetic seawater solution composed of KCl (0.0093 M), NaCl (0.42 M), Na_2SO_4 (0.029 M), $CaCl_2$ (0.011 M), and $MgCl_2$ (0.056 M), as referenced in the reported paper (Nat. Mater. 2022, 21, 1183-1190). As shown in Figure R3, the rejection rates for monovalent and divalent ions reached 99.3% and 99.6%, respectively, indicating exceptional rejection performance in a mixed salt solution.

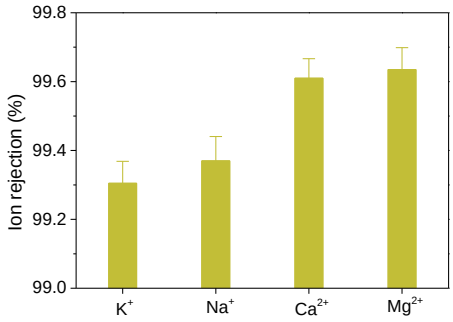

Figure R3. The ion rejection rates of a mix salt solution.

Based on these experimental observation, our membranes demonstrated outstanding desalination performance tested in both 1000 ppm and 35000 ppm of NaCl solution, as well as in mix salt solutions, emphasizing their potential in various desalination contexts, including both brackish and seawater treatment.

3) "The star-shaped configuration allows for more controllable crystallization". However, this requires a more thorough discussion. What does "controllable crystallization under nano-confinement" mean?

Response:

We appreciate the reviewer's comment. Controllable crystallization of star-shaped oligomers under nano-confinement at the air/water interface refers to the precise and organized assembly of star-shaped tetra-PCL-UPy oligomers within the ultrathin membrane thickness (sub 10-nm), facilitated by the unique properties of the star-shaped architecture and the air/water interface. This process is defined by several key aspects:

The nano-confinement in our system refers to the restricted spatial environment provided by the ultrathin membrane, which limits the mobility and arrangement of the star-shaped oligomers. Within a sub 10-nm confined space, molecular motion is restricted, enhancing the organization of the crystalline domains.

The star-shaped architecture features four-armed polycaprolactone (PCL) chains radiating from a central core, with end-functionalized UPy motifs. This geometry ensures that each arm aligns symmetrically, allowing for better spatial control over the crystallization process. The restricted environment further enhances the alignment of these arms, leading to controllable crystallization.

At the air/water interface, the hydrophobic PCL arms repel water, promoting the alignment of the oligomers parallel to the interface, while the polar UPy groups anchor strongly through multivalent hydrogen bonding with water molecules. This interplay ensures that the oligomers are evenly distributed and consistently oriented during the crystallization process, enhancing structural precision.

The organized crystallization within the confined 6-nm thickness directly contributes to the exceptional water permeability and ion rejection performance observed in the membranes. The precise molecular arrangement ensures a uniform pore size distribution and improved fractional free volume in the final membrane structure.

To address this comment, we have expanded the discussion in the Results and Discussion section, emphasizing the role of nano-confinement defined by the ultrathin membrane

thickness and the interplay of molecular interactions at the air/water interface, as stated in paragraph 2, page 4 of the revised manuscript,

"In this study, we strategically designed and synthesized two tetra-oligomers, Tetra-PCL-OH and Tetra-PCL-UPy, featuring identical four-armed crosslinked PCL backbones (Figure 1). Tetra-PCL-OH features hydroxyl terminal groups, while tetra-PCL-UPy is equipped with UPy end-capped units, to explore the importance of the end-group functionalization on the membrane performance. The star-shaped PCL backbones were chosen for their ability to facilitate controllable crystallization in nano-confined environment and to enhance mechanical properties due to their branched architecture. This geometry ensures that each arm aligns symmetrically, providing better spatial control over the crystallization process. The restricted environment provided by the sub-10 nm ultrathin membrane further promotes the alignment of these arms, enabling controllable crystallization. At the air/water interface, the hydrophobic PCL arms repel water, encouraging the alignment of the oligomers parallel to the interface, while the polar UPy groups engage in strong multivalent hydrogen bonding with water molecules. This interplay ensures that the oligomers are evenly distributed and consistently oriented during the crystallization process, enhancing structural precision."

4) "The quadruple hydrogen bonding of UPy motifs enhances the interfacial bonding with water molecules, leading to greater crystalline heterogeneity in the NCC membranes." How do the authors prove this claim?

Response:

We thank the reviewer's thoughtful comment. The strong interaction between UPy ends and water surfaces, combined with the strong water repellency of the PCL backbone, results in a more orderly arrangement of polymer chains in NCC membranes compared to NRC membranes without UPy ends.

To strengthen our argument regarding interfacial hydrogen bonding, we conducted molecular dynamics (MD) simulations for further elucidation. We investigated the interfacial interaction energy between tetra-oligomers and water molecules (Figure 5b). After MD relaxation, we found that the interfacial energy between tetra-PCL-UPy and water molecules (0.2544 kcal $mol^{-1}Å^{-1}$) was greater than that between tetra-PCL-OH and water molecules (0.2034 kcal $mol^{-1}Å^{-1}$) (Figure 5f), indicating strong attractive interactions between tetra-PCL-UPy and H_2O. Moreover, a large number of UPy motifs accumulate at the air/water interface under nano-confinement.

To further elucidate the effect of interfacial hydrogen bonding on the formation of controllable and organized crystallizations in the nano-films, we quantified the number of hydrogen bonds at the nano-confined interface of tetra-PCL-OH/ H_2O and tetra-PCL-UPy/ H_2O. More hydrogen bonds were established at the interface between tetra-PCL-UPy and water molecules, as shown in Figure 5g.

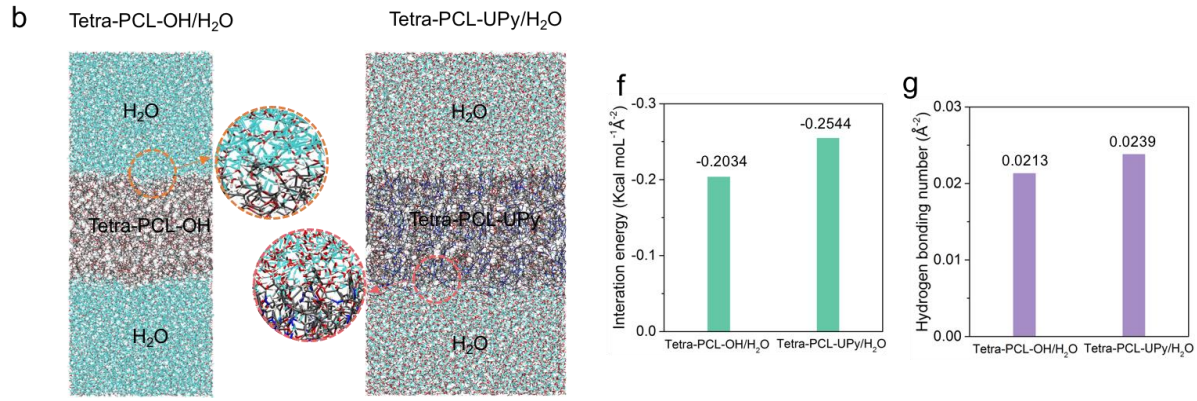

Figure R4. As copy of Figure 5 showed that sandwich models for computing the interactions between tetra-PCL-OH or tetra-PCL-UPy and water molecules, where cyan lines represent the hydrogen bonds formed in the simulation system (b). Areal density of the interaction energy between tetra-PCL-OH or tetra-PCL-UPy and water molecules (f). Areal density of the hydrogen bonds formed between tetra-PCL-OH or tetra-PCL-UPy and water molecules (g).

Due to the interfacial hydrogen bonding interactions, carbonyl groups and UPy motifs at the rear surface of NCC membranes can reconfigurably anchor to water molecules in the nano-confined space, as supported by XPS spectra (Figure 3h). The broad XPS spectrum showed that the percentages of O1s and N1s on the rear surface were greater than those on the top surface, respectively.

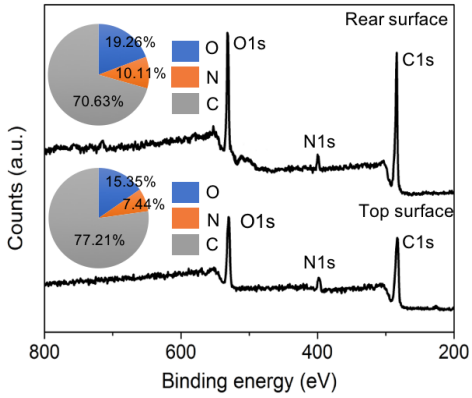

Figure R5. As a copy of Figure 3h of the original manuscript showed the surface XPS spectra of two sides of the NCC-6 membrane.

To substantiate this claim regarding greater crystalline heterogeneity in the NCC membranes, we have conducted a combination of experimental techniques. Raman spectra showed the crystalline peaks of the C-COO stretching band (911 cm^{-1}), C-C stretching band (1108 cm^{-1}), bending band (1441 cm^{-1}) and C=O stretching band (1723 cm^{-1}) on two sides of NCC-6 (Figure 3a). The intensities of the C-C stretching band of the top side are more prominent than those of the rear side, as indicated by Raman mapping (Figure 3b), suggesting the controllable crystallization of the two sides of the NCC-6 membrane. AFM based surface indentations (Figure 3c-f) displayed the modulus profiles and distributions of the two sides of NCC-6 nanofilm. The upper surface displayed a greater abundance of crystals and a significantly higher Young's modulus (approximately 3 GPa) compared to the rear side, aligning with greater crystalline heterogeneity in the NCC membranes. Conversely, both

faces of the NRC-6 membrane exhibited a similar distribution of aggregated regions, as evidenced by the AFM phase images (Figure S18).

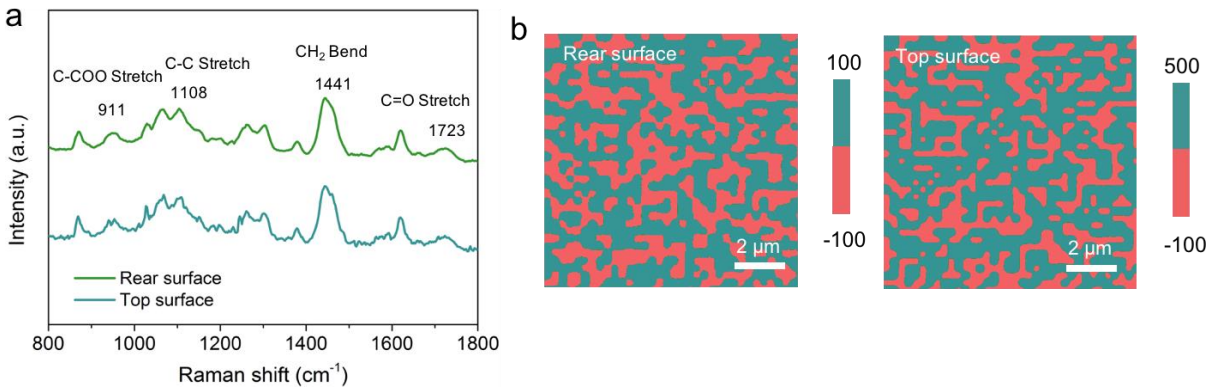

Figure R6. As a copy of Figure 3a-b showed that Raman spectra and mapping of the rear and top surface.

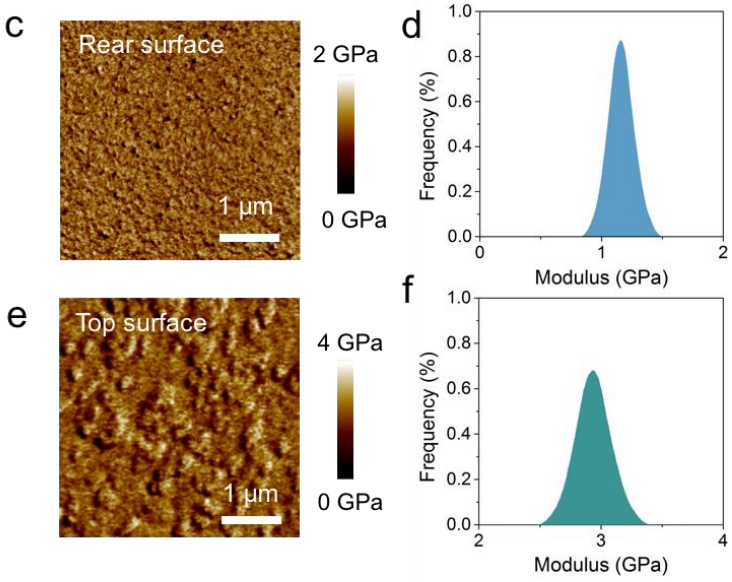

Figure R7. As a copy of Figure 3c-f showed that modulus images and distributions of the rear (c,d) and top (e,f) surfaces of the NCC-6 membrane, as measured by AFM based indentation.

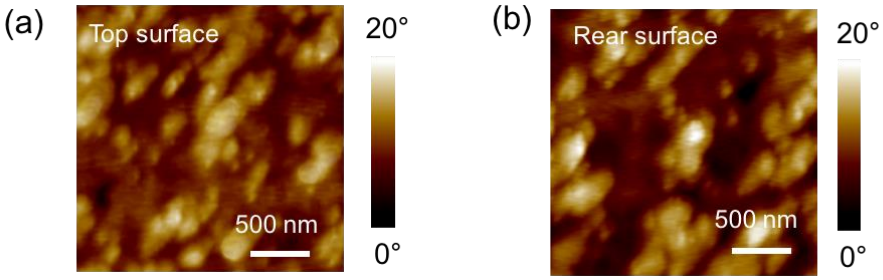

Figure R8. As a copy of Figure S18 showed that AFM phase images of the rear and top surface of the NCC-6 membrane.

Both experimental characterizations and simulations confirm UPy motifs can form strong hydrogen bonding interactions with water molecules, enabling controllable and organized

crystallization within the NCC-series membranes. Also, NCC membranes exhibit greater crystalline heterogeneity than NRC membranes.

5) The membrane NCC-6 was defect-free based on optical microscopy images. This is not the proper characterization technique to make such affirmation.

Response:

We appreciate the reviewer's observation and insightful comment. While optical microscopy offers insights into surface morphology, we agree that it may not be conclusive in characterizing the defect-free nature of the entire membrane. In response to this concern, we have revised the manuscript to clarify the role of optical microscopy (lines 1-2, paragraph 2, page 6 of the revised manuscript),

"The NCC-6 membrane exhibited uniformity with clearly visible edges, as demonstrated by the optical microscope image."

To strengthen our claims regarding the defect-free status of the NCC-6 membrane, we conducted scanning electron microscopy (SEM) characterization. Figure S17 in the original manuscript presents SEM images that confirm the absence of defects on both sides of the NCC-6 membrane when mounted on a silicon wafer, with no significant differences observed.

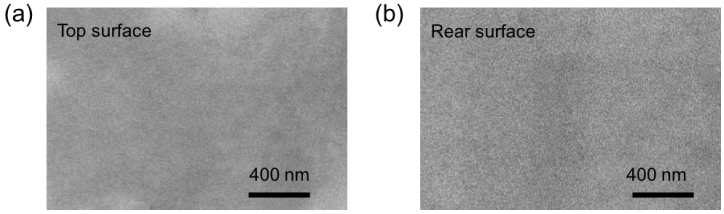

Figure R9. As a copy of Figure S17 showed that SEM images of top and rear surface of the NCC-6 membrane.

We believe that these additional SEM characterizations provide a more robust basis for our claims regarding the defect-free nature of the NCC-6 membrane.

6) "With an increase in solute concentration up to 8 mg mL−1, S slightly increased and reached its maximum value, leading to an initial increase and subsequent decrease in the spreading area of the nanofilms". How do the authors justify this behaviour?

Response:

We thank the reviewer's thoughtful comment. The behavior of the spreading coefficient (S) as a function of solute concentration can be justified as follows:

Role of solute concentration in spreading coefficient (S). The spreading coefficient (S) is influenced by the balance of interfacial tensions between the polymer solution and the water phase. At low solute concentrations, the presence of tetra-PCL-UPy oligomers at the air/water interface lowers the interfacial tension, leading to an increase in S. This promotes the spreading of the nanofilm.

Reaching the maximum spreading area: As the solute concentration approaches 8 mg mL^{-1}, the oligomer molecules saturate the interface, maximizing the reduction in interfacial tension and achieving the largest spreading area. At this point, the spreading is driven by the optimal packing and interactions of the oligomers at the interface.

Reduction in spreading area beyond 8 mg mL^{-1}: Beyond this concentration, further increases in solute concentration lead to the formation of a thicker polymer solution at the interface. This increases the viscosity of the solution, reducing its ability to spread freely. Additionally, excessive solute may lead to aggregation or hinder molecular mobility, thereby limiting the spreading area.

Besides, this behavior aligns with previous studies on interfacial spreading dynamics, where spreading is governed by the interplay between solute concentration, interfacial tension, and solution viscosity (Langmuir 2008, 24, 3185-3190; J. Am. Chem. Soc. 1922, 44, 2665-2685). We have added a more detailed explanation to clarify this mechanism of the revised manuscript (lines 1-6 from the bottom, paragraph 2, page 6; lines 1-4, paragraph 1, page 7),

"The spreading coefficient (S) is influenced by the balance of interfacial tensions between the polymer solution and the water phase. At low solute concentrations, the presence of tetra-PCL-UPy oligomers at the air/water interface lowers the interfacial tension, leading to an increase in S. This promotes the spreading of the nanofilm. As the solute concentration approaches 8 mg mL^{-1}, the oligomer molecules saturate the interface, maximizing the reduction in interfacial tension and achieving the largest spreading area. Beyond this concentration, further increases in solute concentration lead to the formation of a thicker polymer solution at the interface. This increases the viscosity of the solution, reducing its ability to spread freely. Additionally, excessive solute may lead to aggregation or hinder molecular mobility, thereby limiting the spreading area."

7) "As S value decreases, the spreading rate decreases, allowing PCL chains to assemble and crosslink via sufficient folding and orientation. This leads to stronger interactions between polymer chains, resulting in an improved membrane thickness". This is not proven. Furthermore, how could this statement fit with the fact that there was no uniform relationship between diffusion area and crystallinity of NCC membranes?

Response:

We thank the reviewer's valuable feedback. Our statement regarding the relationship between the spreading rate and membrane thickness was intended to convey that a slower spreading rate allow for more time for the polymer chains to assemble and align through sufficient folding. This process leads to stronger interactions between polymer chains, which in turn results in an improved membrane thickness.

To reduce potential confusion, we modified the statement in lines 4-7, paragraph 1, page 7 of the revised manuscript,

"As the spreading parameter (S) decreases, the spreading rate slows, potentially providing more time for PCL chains to interact and align. This may facilitate the folding and orientation of the chains, enhancing inter-chain interactions and contributing to an increase in membrane thickness."

We acknowledge that the relationship between diffusion area and crystallinity is not uniform across all concentrations. We have plotted the relationship between crystallinity and thickness of NCC membranes with increasing solution concentrations (Figure S15). At lower concentrations, we observe a linear increase in thickness alongside increases in both spreading area and crystallinity. Beyond a concentration of 8 mg/mL, while crystallinity continues to rise, the spreading area begins to decrease.

This behavior aligns with our assertion that the decreasing spreading rate potentially provides more time for PCL chains to interact and align, facilitating the folding and orientation of the chains, enhancing inter-chain interactions, and contributing to an increase in membrane thickness and crystallinity. The non-uniform relationship between diffusion area and crystallinity may be attributed to the complex interplay of various factors, including chain folding, orientation, and crosslinking, which can be influenced by the concentration of the solution and the specific properties of the polymer chains.

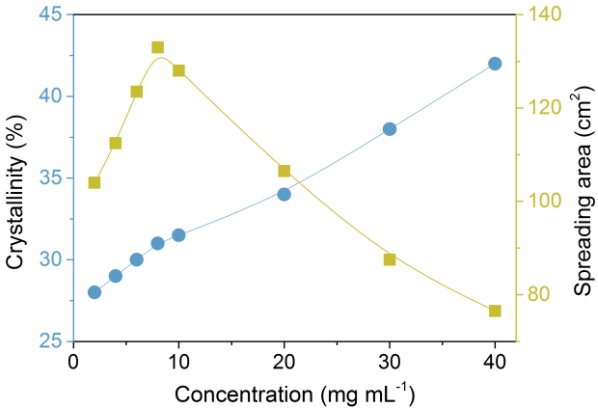

Figure R10. As a copy of Figure S15 showed that the crystallinity and spreading area of NCC membranes with concentrations.

8) "NCC-6 showed a melting temperature of approximately 44°C". How do the Authors comment on the potential real applicability of their membranes with such a low melting temperature?

Response:

We appreciate the reviewer's feedback regarding the melting temperature of NCC-6 and its implications for the real-world applicability of our membranes. We acknowledge that the observed melting temperature of approximately 44°C may raise valid concerns about the thermal stability of the NCC membranes, however, we believe that the operational conditions for many desalination applications, particularly those involving water treatment, typically remain well below this temperature. We have found that commercial polyamide RO membranes like SW30XLE-400 and SEAMAXX-440 show the maximum operating temperature of ~ 45°C. Therefore, the membranes can be expected to function effectively under standard operating conditions.

We have discussed the implications of the melting temperature for practical applications and outlining our ongoing efforts to optimize the thermal properties of the membranes, as indicated in the conclusion and outlook section of the revised manuscript,

"We also acknowledge the limitations of the NCC membranes, which are assembled through non-covalent bonding mechanisms such as hydrogen bonding and hydrophobic interactions, without the benefit of covalently bonded crosslinking. This design choice raises valid concerns regarding the vulnerability of these non-crosslinked membranes to breakdown under high temperatures, solvent exposure, and interactions with surfactants. As the NCC membranes have a melting temperature of approximately 44 °C, their performance may be compromised in applications involving elevated temperatures or aggressive chemical environments. Future work will focus on developing strategies to enhance the thermal and chemical stability of these membranes, potentially through the incorporation of crosslinking

methods or stabilizing additives. Addressing these limitations will be crucial for expanding the practical applicability of NCC membranes in diverse industrial settings."

9) The authors reported that, compared to the NRC-6 membrane, the NCC-6 membrane had a narrower pore size. How is this demonstrated? What about the statistical validity of such data?
Response:
We sincerely thank the reviewer's comment regarding the demonstration of pore sizes between the NRC-6 and NCC-6 membranes.

In our study, we utilized both Molecular Weight Cut-Off (MWCO) solute rejection experiments and molecular dynamics (MD) simulations to estimate and compare the pore sizes of the two membranes. These two independent methods yielded consistent results. Specifically, the MWCO data (Figure R2) indicated pore radii of 0.28 ± 0.08 nm for the NCC-6 membrane and 0.36 ± 0.11 nm for the NRC-6 membrane. Similarly, the MD simulations (Figure R1) provided simulated pore radii of 0.27 ± 0.07 nm for NCC-6 and 0.35 ± 0.14 nm for NRC-6.

To ensure the robustness and statistical validity of our findings, we have elaborated on the methodologies and statistical analyses used. In particular, we added a detailed explanation in the paragraph three from the bottom of page 16 in the Supplementary Information (SI), which states:

"For MD simulations, to mitigate statistical fluctuations and ensure result validity, we conducted an additional 2 ns of simulations after reaching equilibrium. Molecular configurations within the simulation boxes were gathered every 100 ps for density calculations and void analysis. Each simulation was repeated independently three times, and the averaged values from these trials were used to obtain robust and reliable data, ensuring the precision and statistical stability of the results."

These measures were implemented to provide precise and reliable data supporting our conclusion regarding the narrower pore size of the NCC-6 membrane compared to the NRC-6 membrane. We appreciate the reviewer's comment and trust that this additional clarification addresses their concern.

10) "The intensities of the C-C stretching band of the top side are more prominent than those of the rear side, as indicated by Raman mapping (Figure 3b), suggesting the controllable crystallization of the two sides of the NCC-6 membrane". This is rather speculative and need further demonstration.
Response:
We appreciate your concern regarding the interpretation of the Raman mapping data. The C-C stretching band in the Raman spectrum is associated with the crystalline structure of polycaprolactone (PCL), as referenced in the literature (Polymer, 2017, 117, 1-10; J. Am. Chem. Soc. 2022, 144, 14278-14287; J. Mol. Struct. 2020, 1215, 128294). As observed in Figure R10, which is derived from Figure 3a-b of the original manuscript, the intensity of this band is stronger on the top surface compared to the rear surface, indicating more ordered crystalline regions on the top side.

To further support our claim regarding about the controllable crystallization on both sides of the NCC-6 membrane, we conducted additional experimental evidence and detailed analysis

of AFM surface indentation measurements, as indicated in Figure R5 (copied from Figure 3c-f of the original manuscript),

"AFM based surface indentations (Figure 3c-f) displayed the modulus profiles and distributions of the two sides of NCC-6 nanofilm. The upper surface displayed a greater abundance of crystals and a significantly higher Young's modulus (approximately 3 GPa) compared to the rear side, aligning with the controlled and organized crystallization observed in the NCC membrane."

Therefore, these observations and experimental evidence strengthen our argument regarding controllable crystallization between the two surfaces of the NCC-6 membrane.

11) The authors explained that the Janus wetting properties and chemical heterogeneity of the two sides of the NCC membranes were due to the carbonyl groups and the orientation of the Upy motif at the water/air interface. However, this type of orientation should also occur, albeit to a lesser extent, with NRC samples. Why didn't this kind of orientation occur at all in the latter case? This should be commented.

Response:

We appreciate the reviewer's careful observation and insightful comment. We agree with the reviewer that the NRC sample should exhibit less pronounced Janus properties. The polar motifs can migrate to the sides in contact with the water molecules, enabling surface chemical reconfiguration in the nano-confined space, due to hydrogen bonding interactions.

The NCC membranes incorporate UPy motifs, which possess strong hydrogen bonding capabilities that promote a more pronounced chemical heterogeneity and Janus wetting properties on the rear surface. In contrast, the NRC samples lack UPy motifs and only feature carbonyl groups, resulting in a less obvious Janus properties. This is because the relatively weak hydrogen bonding interactions between water molecules and carbonyl groups lead to limited surface reconfiguration.

As indicated in Figure S19 of the original SI, the water contact angle of the rear surface of the NRC membrane is comparable to that of the top surface.

To enhance clarity and address the reviewer's concerns, we have modified the statement regarding the NRC sample (lines 6-8, paragraph 2, page 9):

"However, for NRC-6 membrane, WCA of the top side is slightly higher than that of the rear side, indicating less pronounced Janus wetting properties (Figure S19)."

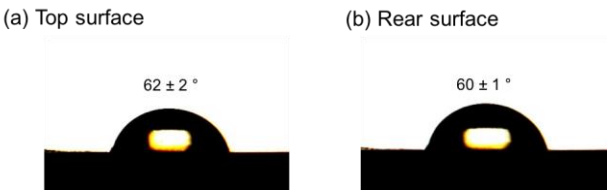

Figure R11. As a copy of Figure S19 showed that water contact angles of two sides of the NRC-6 membrane.

12) On page 11, the authors stated that their membranes outperformed current state-of-the-art RO membranes. However, they forget to specify under which test conditions the membranes

were tested, especially considering the salt concentration used in their tests (1000 ppm and single salt).

Response:

Thank you for highlighting this important aspect. We recognize that specifying the test conditions is crucial for contextualizing our performance claims compared to state-of-the-art reverse osmosis (RO) membranes. To enhance the clarity and rigor of our manuscript, we have specified the test conditions in detail, including the salt concentration of 1000 ppm and the use of a single salt, as noted on page 11 of the revised manuscript,

"As indicated in Figure 4e, the NCC-6 membrane demonstrated a high water permeance (14.8 L m^{-2} h^{-1} bar^{-1}) and an exceptional water/NaCl selectivity (54 bar^{-1}) when tested with a 1000 ppm NaCl solution at 10 bar, outperforming the upper bound of water/NaCl selectivity observed in the current state-of-the-art RO and NF membranes."

13) It is possible to discuss "Long-term RO separation measurements" when RO refers to a solution diffusion transport mechanism, that is typical of dense membranes (or with interspace of polymer chains in the order of a few Angstroms). What about the transport mechanism in such membranes? (also, in connection to the observed rejection of boron).

Response:

We appreciate the reviewer's insightful comment regarding the transport mechanisms involved in our membranes.

We have evaluated and discussed the 168-h desalination performance with a 1000 ppm NaCl solution at 10 bar, as stated in Figure 4f of the original manuscript,

"The NCC-6 membrane maintained a high NaCl rejection rate over 99% for the initial 120-h operation and reached 98.6% with a total duration of 168 h, while the water flux slightly decreased by 8.3%, possibly due to concentration polarization."

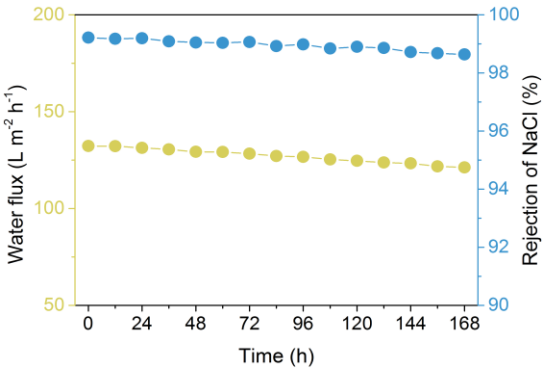

Figure R12.As a copy of Figure 4f showed that 168-h desalination performance of the NCC-6 membrane treated with a 1000 ppm NaCl solution at 10 bar.

Regarding the transport mechanism of water and salt through the NCC membrane, we conducted molecular dynamics simulation. The equilibrium structure of each system revealed that the specific orientation of PCL chains in the crystalline domains facilitates the formation of continuous water channels (Figure R13, a to d), enabling uninterrupted water transport and high water flux. We also calculated the number of water molecules transferred across the

NCC membrane during the final 15 ns of the desalination process (Figure R19e). The water flux in the crystalline domains was approximately 2.86 molecules/ns.

[Redacted]

Figure R13. Equilibrium structure of the system with the crystalline regions (a) and the continuous water channel formed (b-d). Continuous water channel in crystalline regions results in continuous water transport in desalination process. (e) Number profiles of water molecules transferred across membranes with crystalline structures during desalination process.

To explain the experimental observations of improved ion rejection performance, we calculated the potential of mean forces profiles (PMF) for sodium ion transport from the center to the edge of the membrane (Figure R14a). The PMF profiles showed that the sodium ion transport needs to overcome a higher energy barrier in the crystalline regions, leading to better ion rejection performance. To further investigate the ion transport mechanisms, we captured the ion solvation structures during sodium ion transport across the membrane (Figure R14b). The evolution of the ion solvation structure during transport revealed that more oxygen groups replace the water solvation with sodium at both the ends and the middle of the crystalline domains because of the structural features of the units. Consequently, sodium ions must disrupt the solvation structure between the polymer chains and sodium ions, facing a higher energy barrier in the oriented channels within the crystalline regions.

[Redacted]

Figure R14. (a) Potential of the mean force profiles for sodium ion transporting from membrane center to the membranes entrance. (b) Evolution of sodium ion solvation structures during transport across crystalline regions.

Commercial RO membranes typically exhibit low boron rejection due to the small molecular weight of neutral H_3BO_3 (61.8 g/mol). In our study, the controlled assembly and crystallization of the NCC membranes reduce pore size and refine the pore radius distribution (0.28 ± 0.08 nm), thereby enhancing the rejection of small boron solutes. For neutral H_3BO_3 at pH 7, the NCC-6 membrane demonstrated a rejection rate of approximately 75%. Under basic conditions, this rejection rate increased to over 98% for the anionic $B(OH)_4^-$ at pH 10.

14) The surface roughness of the NCC-6 membranes and their greater resistance to harsh conditions compared to the NRC-6 sample is unclear.

Response:

We appreciate the reviewer's comment regarding the surface roughness of the NCC-6 membranes and their resistance to harsh conditions compared to the NRC-6 sample.

In our initial studies, we measured surface roughness of the NCC-6 membrane (Figure 2c), and investigated its resistance to harsh conditions, as indicated in Figure S32-34. The NCC-6 membranes were immersed in acid (pH 3), base (pH 11), and a urea solution (1 wt%), respectively, for 24 hours, after which they were removed and thoroughly cleaned with DI water and air-dried for subsequent measurements.

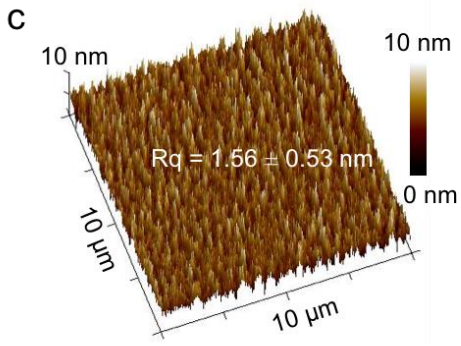

Figure R15. As a copy of Figure 2c showed the roughness of NCC-6 membrane.

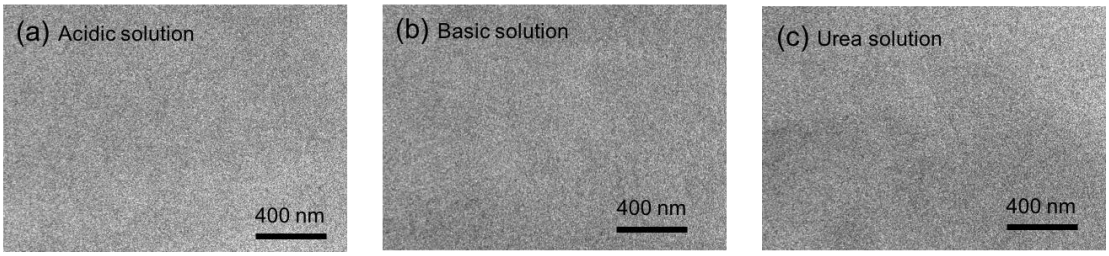

Figure R16. As a copy of Figure S32 showed that SEM images of NCC-6 membranes that was treated with acidic (pH = 3), basic (pH = 11), and urea (1 wt%) solutions for 24 hours.

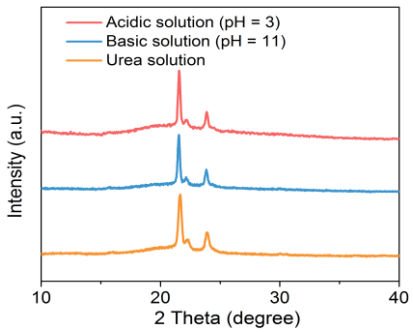

Figure R17. As a copy of Figure S33 showed that XRD profiles of NCC-6 membranes that was treated with acidic (pH = 3), basic (pH = 11), and urea (1 wt%) solutions for 24 hours.

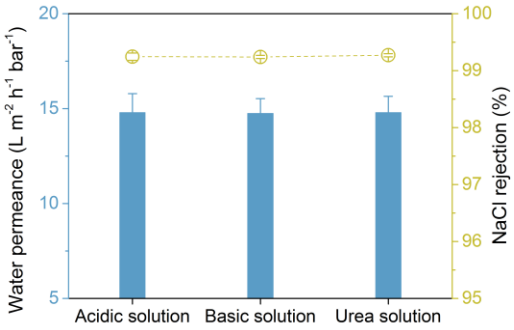

Figure R18. As a copy of Figure S34 showed that water permeance and NaCl rejection of NCC-6 membranes that was treated with acidic (pH = 3), basic (pH = 11), and urea (1 wt%) solutions for 24 hours.

To further address the reviewer's concern, we have conducted additional experiments to measure the surface roughness of the NRC-6 membrane (Figure R19) and to assess its resistance to the same harsh conditions using the same methods, as indicated in Figure R20. Our results show that the NRC-6 membrane has a root mean square roughness of 1.75 ± 0.32 nm for an area of 10 × 10 μm, along with structural and desalination stability under three harsh conditions tested.

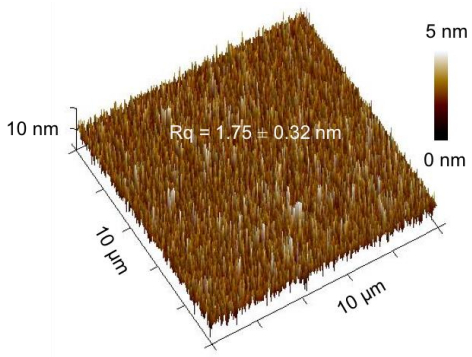

Figure R19. Surface roughness of the NRC-6 membrane.

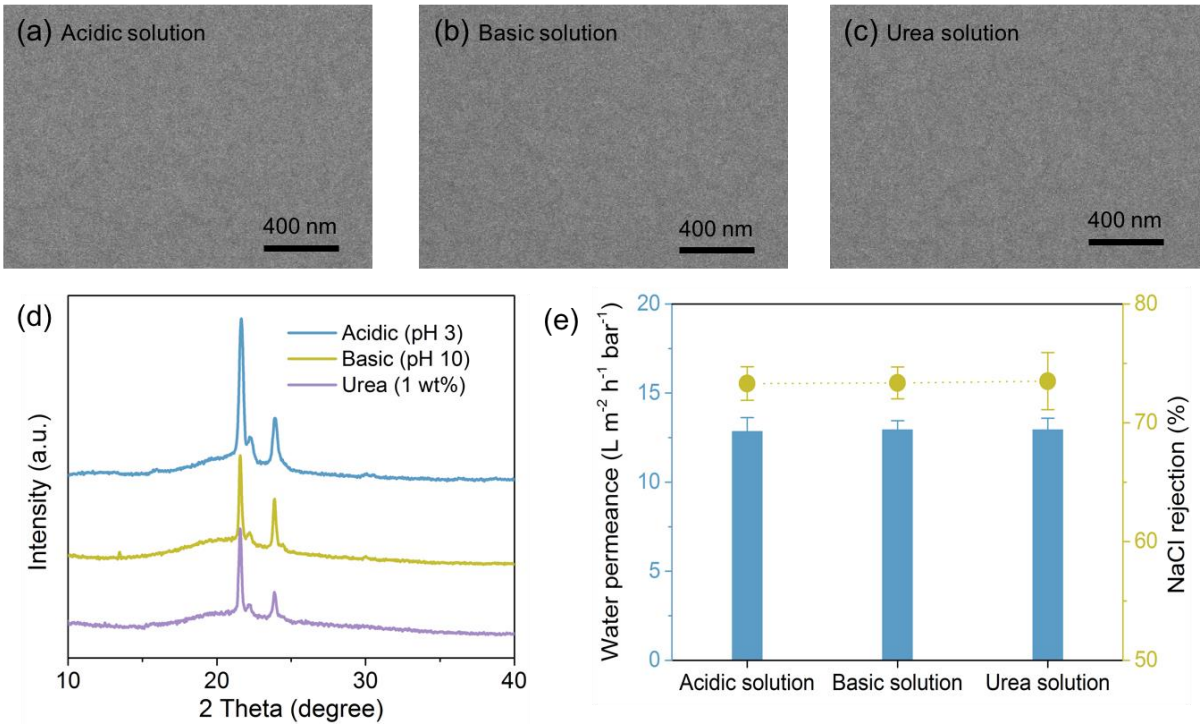

Figure R20. (a-c) Morphological properties of the NRC-6 membranes treated with acid (pH 3), base (pH 11), and urea (1 wt%) for 24 hours; (d) XRD profiles of the NRC-6 membranes treated with acid (pH 3), base (pH 11), and urea (1 wt%) for 24 hours; (e) The water permeance and NaCl rejection of the NRC-6 membrane treated with acid (pH 3), base (pH 11), and urea (1 wt%) for 24 hours.

Based on these experimental observations, both the NCC-6 and NRC-6 membranes exhibit low surface roughness and strong resistance to harsh conditions, highlighting their robustness and suitability for challenging applications.

15) More importantly, the authors reported the highest permeability (14.8 L m-2 h-1 bar-1H) and water/NaCl selectivity (54 bar-1) among current state-of-the-art RO membranes. However, in addition to not specifying the test conditions (in particular the concentration and temperature of the feed), they carried out this calculation based on weight data from a system of 3 cm2 active membrane area. Using such tiny equipment means using small feed and permeate volumes, small tube diameters, and small sensors and scales to measure the increase in permeate weight. On such a small scale, the indeterminacy of a single drop of water could make a big difference, heavily influencing the calculated transmembrane flux. Why didn't the authors use larger membranes to confirm what they obtained on such a small scale? What about the scalability of the method?

Response:

We thank the reviewer for their thoughtful comments and for highlighting important aspects of our experimental methodology.

To clarify, the reported permeability of 14.8 LMH/bar and water/NaCl selectivity of 54 bar^{-1} were obtained under the specific test condition: a feed concentration of 1000 ppm NaCl, at a pressure of 10 bar, and room temperature (approximately 25°C), as specified in paragraph 2, page 11 of the revised manuscript.

The choice of a 3 cm^2 active membrane area was primarily for initial proof-of-concept studies. We recognize the limitations inherent in small-scale testing and fully appreciate the concerns regarding measurement precision and the potential impact of small volume variations on calculated transmembrane flux. To address these concerns, we have conducted further experiments using larger areas of NCC membranes. As indicated in Figure R21, both larger membranes of 12.6 cm^2 and 19.6 cm^2 demonstrate comparable the water flux and rejection rates to those observed with the 3 cm^2 membrane, tested under the same conditions.

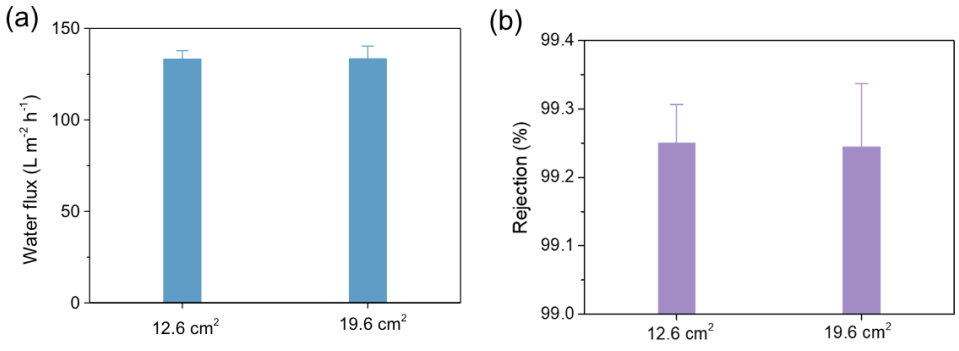

Figure R21. Water flux and rejection with a larger membrane at a 1000 ppm NaCl solution and 10-bar pressure.

Our current research focuses on a novel concept that uses multivalent H-bond interactions at the nano-confined space. This innovative approach aims to control and organize crystallization selectively, which, as we have demonstrated, can significantly refine pore size

distribution, resulting in ultra-selectivity and enhanced water transport. It is important to clarify that our current emphasis is on the fundamental understanding and proof-of-concept of this new mechanism, rather than on immediate industrial scalability. We believe that the principles and findings presented here lay the groundwork for future studies that can develop scalable fabrication methods. We are committed to exploring strategies to ensure the scalability in the next stages of our research.

Reviewer #2 (Remarks to the Author):

The manuscript demonstrates polymeric membranes formed by controllable crystallization of oligimers. The material introduced in the work shows better permeability-selectivity performance than the polyamide-based membranes widely used for desalination. The membrane also appears to be robust under pressure, tolerate some chlorine exposure, and operate after exposure to harsh pH conditions. Overall, the work is impressive and demonstrates what appears to be a feasible chemistry to improve upon long-standing polyamide membranes. My main criticisms relate to the lack of comparisons in performance to conventional polyamide membranes and difficulty understanding the transport mechanisms in this system. Comments are further expanded upon below.

Response:

We would like to express our gratitude for the reviewer's positive feedback and acknowledgment of the potential of our polymeric membranes formed through controllable crystallization of oligomers. We sincerely appreciate the reviewer raising valid concerns about the comparison between our membranes and conventional polyamide membranes and the proposed mechanism in our manuscript. Below, we have carefully addressed each of the detailed concerns put forth by the reviewer.

1. The authors emphasize strong hydrogen bonding in the abstract and also discuss the void size in molecular simulations. However, the proposed rejection mechanisms in this membrane remain unclear. The authors should consider adding a clearer discussion of rejection mechanisms so that readers can better understand which compounds are likely to be rejected and which compounds will pass through these membranes.

Response:

We appreciate the reviewer's valuable feedback regarding the rejection mechanism. This study allows for precise molecular arrangement at air/water interfaces, enabling controllable crystallization and minimizing pore size distribution, which achieves a water-mono-ions selectivity of over 54 bar^{-1}.

To enhance the clarity and better understand the transport mechanism, we have done molecular dynamics simulations. The equilibrium structure of each system revealed that the specific orientation of PCL chains in the crystalline domains facilitates the formation of continuous water channels (Figure R22, a to d), enabling uninterrupted water transport and high water flux. We also calculated the number of water molecules transferred across the NCC membrane during the final 15 ns of the desalination process (Figure R22e). The water flux in the crystalline domains was approximately 2.86 molecules/ns.

[Redacted]

Figure R22. Equilibrium structure of the system with the crystalline regions (a) and the continuous water channel formed (b-d). Continuous water channel in crystalline regions results in continuous water transport in desalination process. (e) Number profiles of water molecules transferred across membranes with crystalline structures during desalination process.

To explain the experimental observations of improved ion rejection performance, we calculated the potential of mean forces profiles (PMF) for sodium ion transport from the center to the edge of the membrane (Figure R23a). The PMF profiles showed that the sodium ion transport needs to overcome a higher energy barrier in the crystalline regions, leading to

better ion rejection performance. To further investigate the ion transport mechanisms, we captured the ion solvation structures during sodium ion transport across the membrane (Figure R23b). The evolution of the ion solvation structure during transport revealed that more oxygen groups replace the water solvation with sodium at both the ends and the middle of the crystalline domains because of the structural features of the units. The transport of sodium ions requires the disruption of the solvation structure between the polymer chains and sodium ions. As a result, sodium ions need to overcome a higher energy barrier in the oriented channels within crystalline regions.

[Redacted]

Figure R23. (a) Potential of the mean force profiles for sodium ion transporting from membrane center to the membranes entrance. (b) Evolution of sodium ion solvation structures during transport across crystalline regions.

Based on our experimental observations and simulations, the well-aligned crystalline channels facilitate rapid water transport, resulting in high water flux. At the same time, these channels increase the energy barrier for sodium ion transport, which leads to a high rejection rate of sodium ions.

2. I would assume that the presence of a crystalline region (which does not allow for water flow) would decrease the effective membrane area, since only the amorphous regions are accessible to water. Can the authors estimate the accessible/active pore area? It is surprising the permeability can be so high with some of the pore area blocked off (e.g., compared to conventional RO membranes which presumably do not have similar impermeable regions).
Response:
We thank the reviewer's thoughtful comment. We would like to clarify that well-aligned crystalline channels in the NCC membranes facilitate rapid water transport while providing high ions rejection.

To evaluate the accessible fractional volume and pore diameter, we constructed structural models, representing the NCC membrane and the NRC membrane, respectively, as shown in Figure 5c. In contrast to the NRC membrane derived from tetra-PCL-OH, the NCC membrane fabricated by tetra-PCL-UPy exhibited a narrower distribution of pore sizes (Figure 5d) and a higher fractional free volume (Figure 5e). These findings are consistent with experimental characterizations (Figure S16) and support our claim of the controllable crystallization in the NCC membrane that can refine the pore size distributions.

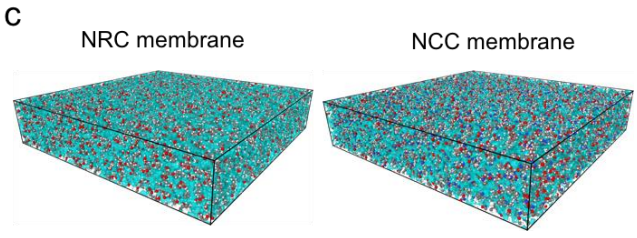

Figure R24. As a copy of Figure 5c showed that the free volume in NRC and NCC (see the space occupied by translucent light green volume) detected by a theoretical probe with a radius of 1 Å.

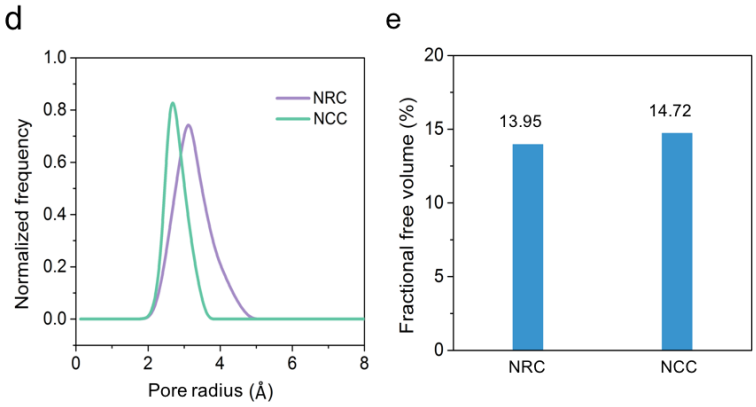

Figure R25. As a copy of Figure 5d-e showed that the simulated pore size and the fractional free volume.

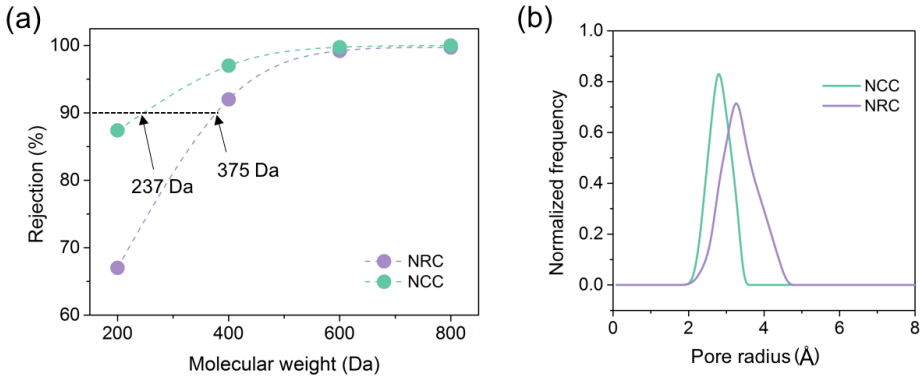

Figure R26. As a copy of Figure S16 showed that the experimental pore size distributions of the NCC-6 membrane.

In our work, the NCC-6 membranes feature hydrophilic surface (Figure R27), negatively charged surface (Figure R28), and improved fractional free volume (Figure R25). Synergistically, the water permeability coefficient (A value) of the NCC-6 was ~ 14.8 LMH/bar, substantially higher than that of the commercially available seawater desalination membranes (≈1.5 LMH/bar).

Figure R27. As a copy of Figure 3g in the revised manuscript showed WCA of two sides of NCC-6 membrane.

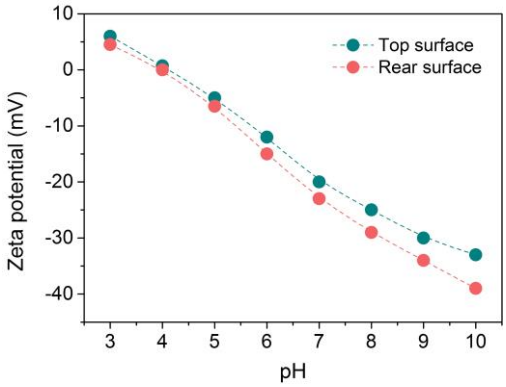

Figure R28. As a copy of Figure S21 in the original SI showed surface zeta potentials of two sides of NCC-6 membrane.

3. I did not understand why the shape of the oligomers would result in channels. Since they are end-capped with hydrogens bonds, it seems like the center of a repeating circle would be impermeable and the outside would be permeable.

Response:

We thank the reviewer's concerns regarding the relationship between the shape of the oligomers and the formation of channels in the membrane. The star-shaped tetra-PCL-UPy oligomers feature a four-armed polycaprolactone (PCL) structure with UPy motifs at the termini of each arm. During the self-assembly process at the air/water interface, the PCL backbones tend to orient away from the water phase, while the polar UPy groups engage in strong hydrogen bonding interactions with water molecules. This interaction drives the alignment of the oligomers into an ordered and controllable crystallization, refining distribution of pore sizes for ultra-selectivity and boosting the available space for fast water transport.

Furthermore, the precise assembly and orientation of the PCL chains in the controlled crystallization regions create abundant subnanometer channels that facilitate fast water transport, as demonstrated by our molecular dynamics simulations (Figure R22).

4. Although the membranes appear to be sufficiently robust for operation under high pressure and proof-of-concept testing, they are not crosslinked. This would make them vulnerable to breakdown at high temperature (I think the authors say NCC-6 melts around 44 °C), after solvent exposure, or possibly after exposure to surfactants. The authors should comment on limitations or areas for future work in terms of membrane robustness.

Response:

We appreciate the reviewer for bringing this important point to our attention. The NCC membranes are assembled by non-covalent bonding such as hydrogen bonding and hydrophobic interactions, without covalent bonded crosslinking. This raise valid concerns about the vulnerability of non-crosslinked membranes to breakdown under high temperatures, solvent exposure, and surfactant interactions.

To provide a more comprehensive discussion of our membranes, we have added the potential limitation and future directions to the conclusion and outlook section of the revised manuscript,

"We also acknowledge the limitations of the NCC membranes, which are assembled through non-covalent bonding mechanisms such as hydrogen bonding and hydrophobic interactions, without the benefit of covalently bonded crosslinking. This design choice raises valid concerns regarding the vulnerability of these non-crosslinked membranes to breakdown under high temperatures, solvent exposure, and interactions with surfactants. As the NCC membranes have a melting temperature of approximately 44 °C, their performance may be compromised in applications involving elevated temperatures or aggressive chemical environments. Future work should focus on developing strategies to enhance the thermal and chemical stability of these membranes, potentially through the incorporation of crosslinking methods or stabilizing additives. Addressing these limitations will be crucial for expanding the practical applicability of NCC membranes in diverse industrial settings."

5. During fabrication of the films, what determines thickness? Intuitively the droplet in chloroform should continue spreading to make a very thin film. Was uniform thickness observed through the sample?

Response:

We thank the reviewer's insightful comment. The membrane thickness formed by microdroplet spreading on a water interface is primarily influenced by spreading coefficient. As illustrated in Figure S10a of original SI, the spreading coefficient (S) governs the behavior of the polymer microdroplets deposited and spread at the air/water interface, following the equation $S = \gamma_1 - \gamma_2 - \gamma_{12}$, where γ_1 and γ_2 are the surface tension of the water and the polymer solution, respectively, and γ_{12} is the interfacial surface tension between the two (Langmuir 2008, 24, 3185-3190; Langmuir 2017, 33, 14766-14771; J. Colloid Interface Sci. 2023, 641, 299-308). S determines whether the microdroplet will spread at the water surface and the spreading status, *e.g.* speed, area and thickness. A positive spreading coefficient promotes spreading, leading to a thinner film.

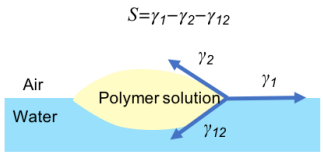

Figure R29. As a copy of Figure S10a of the SI showed the spreading coefficient (S) that governs the behavior of the microdroplets spread at the air/water interface.

We acknowledge the reviewer that the droplet in chloroform should continue spreading to make a very thin film, as evidenced by Figure 2b of the original manuscript. Additionally, the NCC-6 membrane exhibited a uniform surface over an area of 10 × 10 μm, with a low root mean square roughness (Rq) of 1.56 nm, as indicated in Figure 2c.

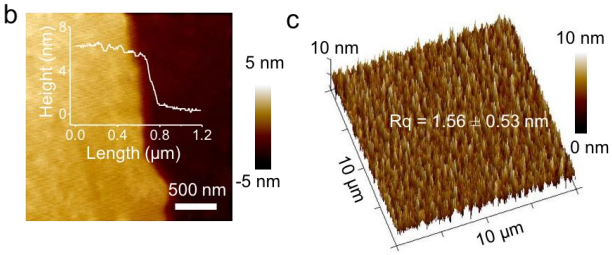

Figure R30. As a copy of Figure 2b-c showed that the membrane thickness profile of 6.2 ± 0.5 nm and the uniform roughness of the NCC-6 membrane.

We further investigated the thickness of the NCC-6 membrane, tested every 1 mm from the center to the edge (Figure R31). The membrane thickness remains constant at the center of the film, and then decreases towards the edge. In the context of a droplet spreading at the air/water interface, the spreading dynamics can be influenced by the surface tension gradient, which may lead to non-uniform film thickness due to the differential in surface tension forces across the film.

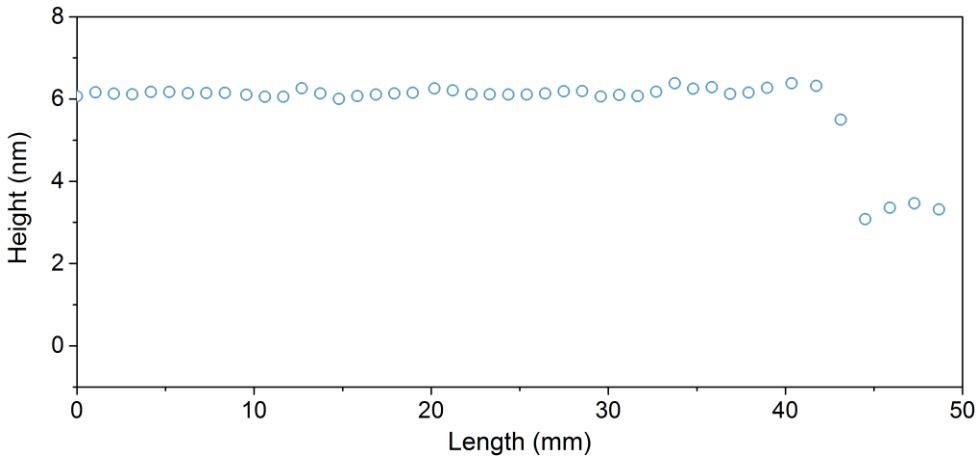

Figure R31. The thickness scatter plot of the NCC-6 membrane tested every 1 mm from the center to the edge.

Based on the experimental observations, the spreading coefficient plays a critical role in determining membrane thickness during the spreading of microdroplets on the water surface. The resultant NCC membrane has uniform thickness with a low roughness value, confirming the consistency of the film at a small scale. Also, the membrane thickness remains constant at the center of the film, and then decreases towards the edge.

6. Why was long-term testing conducted at only 4 bar? Is long-term pressure stability difficult for these membranes?

Response:

We appreciate the reviewer's careful reading and for highlighting this important aspect. We would like to clarify that long-term testing was conducted with a 1000 ppm NaCl solution at 10 bar, rather than 4 bar, as specified in the caption of Figure 4f of the original manuscript. We sincerely apologize for any confusion caused by typographical errors.

To evaluate the long-term desalination stability, we monitored 168-h desalination performance, as shown in Figure 4f of the original manuscript,

"The NCC-6 membrane maintained a high NaCl rejection rate over 99% for the initial 120-h operation and reached 98.6% with a total duration of 168 h, while the water flux slightly decreased by 8.3%, possibly due to concentration polarization."

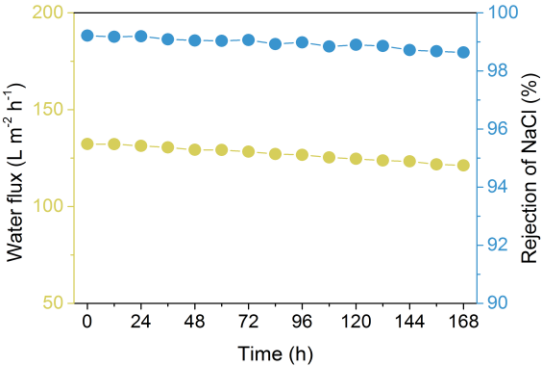

Figure R32.As a copy of Figure 4f showed that 168-h desalination performance of the NCC-6 membrane treated with a 1000 ppm NaCl solution at 10 bar.

Additionally, morphological and structural assessments confirm that the integrity of the membranes remained intact after 168-h testing at 10 bar, as indicated in Figures S26-28.

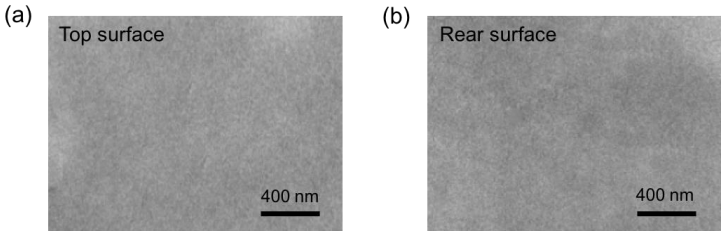

Figure R33. As a copy of Figure S26 showed that SEM images of the NCC-6 membrane with two sides after 7-day desalination with 1000 ppm NaCl solution at 10 bar.

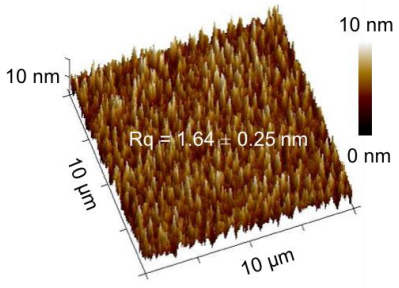

Figure R34. As a copy of Figure S27 showed that AFM roughness profile of the NCC-6 membrane after 7-day desalination with 1000 ppm NaCl solution at 10 bar.

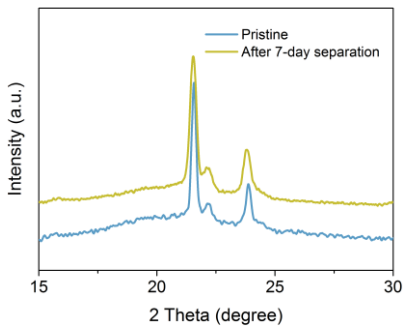

Figure R35. As a copy of Figure S28 showed that XRD images of the NCC-6 membrane after 7-day desalination with 1000 ppm NaCl solution at 10 bar.

Based on these results, we believe our membranes exhibit strong long-term pressure stability.

7. The boron rejection did not appear to be particularly high. Comparison to equivalent polyamide reverse osmosis membranes may be helpful for context.
Response:
We appreciate the reviewer's valuable feedback and suggestions regarding the boron rejection performance. In our initial studies, we observed that the boron removal rates of NCC-6, NCC-12 and NCC-18 were 75%, 88.5% and 93.4%, respectively, under a neutral condition at 5 ppm boron concentration and 10 bar.

To enhance our analysis, we performed boron rejection measurements of the NCC membranes alongside commercial polyamide RO membranes including SW30XLE-400, SEAMAXX-440, under the same testing conditions, e.g., 5 ppm boron solution, pH 8 and 15-bar pressure. We have included these comparative results in Figure R36 to provide a clearer context for the performance of our membranes.

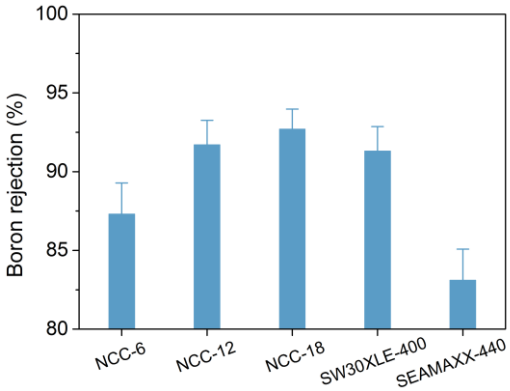

Figure R36. Comparison of boron rejection between our membranes and commercial polyamide RO membranes under the same testing conditions.

Based on the experimental observations, the NCC-18 membrane achieves a maximum boron rejection. Overall, and the boron rejections of our NCC membranes are greater than or comparable to those of the commercial polyamide RO membranes.

8. I found the chlorine and pH exposure results interesting and impressive. You may include results for conventional polyamide membranes here for context. We have found these decrease to around 50% rejection after exposure to similar chlorine doses.
Response:
We are grateful for the reviewer's positive feedback on the chlorine and pH exposure results. We are glad to hear you found them interesting and impressive. We appreciate your suggestion to include comparative results for conventional polyamide membranes.

To provide context, we have incorporated a comparison of our membrane and commercial polyamide membranes under the same testing conditions, as indicated in Figure R37. With the treatment of acidic solution (pH = 3) and basic solution (pH = 11) for 24 hours, the NaCl rejection rates of NCC-18 membrane remain unchanged and are higher than those of commercial polyamide membranes.

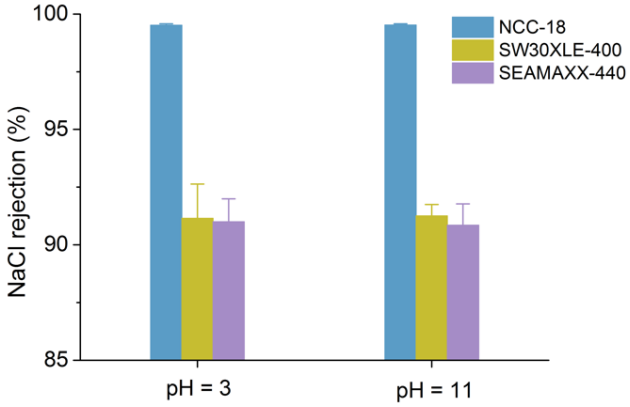

Figure R37. NaCl rejection of NCC-18 and commercial polyamide membranes treated with various solution of pH =3 and pH = 11, using the following experimental conditions: The membranes were soaked in acidic or basic solution under continuous stirring at 25°C. After 24 hours, the membranes were removed from the solution, rinsed thoroughly with deionized water, and tested for their desalination performance with following experimental conditions: an effective membrane area of 12.6 cm^2, 1000 ppm NaCl feed solution, cross-flow rate of 4 L/min, a constant pressure of 10 bar.

When treated with a chlorine solution (200 ppm) for 24 hours (total chlorine: 4800 ppm h) at various pH conditions, NCC-18 membrane shows comparable and high NaCl rejection over all pH ranges (Figure R38), in contrast to untreated sample. However, commercial polyamide membranes feature low NaCl rejection rates of ~55% at pH = 5, ~67% at pH = 7, and ~70% at pH =9. Therefore, this comparison highlights the resilience of our NCC membranes under harsh conditions.

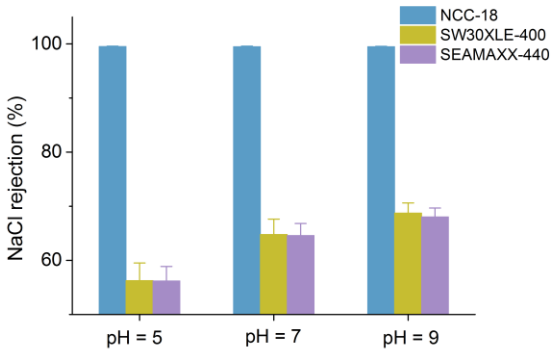

Figure R38. NaCl rejection of NCC-18 and commercial polyamide membranes treated with NaClO solution at various pH solutions, using the following experimental conditions: The membranes were soaked in NaClO solution under continuous stirring at 25°C, and the solution pH was adjusted to the set values. The total chlorine exposure amount was 4800 ppm h (200 ppm NaClO solution for 24 hours). After 24 hours, the membranes were removed from the solution, rinsed thoroughly with deionized water, and tested for their desalination performance with following experimental conditions: an effective membrane area of 12.6 cm^2, 1000 ppm NaCl feed solution, cross-flow rate of 4 L/min, a constant pressure of 10 bar.

This comparison underscores the superior resilience of our NCC membranes under harsh conditions, including chlorine exposure, which is a common challenge for polyamide membranes. Polyamide membranes are known to degrade when exposed to chlorine, as

chlorine can break down the amide groups in the polyamide structure, leading to reduced effectiveness in removing salt and other impurities. Our NCC-18 membrane's performance is particularly impressive given that conventional polyamide membranes typically see a decline in rejection to around 50% after exposure to similar chlorine doses.

In summary, the enhanced stability and performance of our NCC-18 membrane under chlorine and pH exposure demonstrate its potential for applications where membrane integrity under such conditions is critical, outperforming conventional polyamide membranes.

9. Page 12, last paragraph: I did not understand comparison to the NRC-6 membranes rather than other polymeric desalination membranes.

Response:

We thank the reviewer's insightful comment. We would like to clarify that our intention in comparing the NCC membranes with the NRC-6 membranes was to highlight our unique design concept of our NCC membrane. Specifically, the NCC membrane uses multivalent H-bond interactions of tetra-PCL-UPy oligomers at the air/water interface to manipulate nano-confined supramolecular assembly, leading to controllable and organized crystallization. This arrangement can effectively narrow the distribution of pore sizes for ultra-selectivity and boosts the available space for rapid water transport.

To explore the significance of the end-group UPy motifs and their strong hydrogen bonding on the performance of the NCC membrane, we chose the NRC membrane made from tetra-PCL-OH as a control sample. This allowed us to conduct a series of comparative analyses between the NCC and NRC membranes.

Based on the reviewer's suggestion, we have also performed comparative studies of our membranes and commercial polyamide membranes, including evaluations of boron rejection as well as chlorine and pH exposure resistance, as indicated in Figure R36-38. These additional comparisons strengthen the depth and comprehensiveness of our work.

10. "The nanofilm adheres firmly to the substrate due to the high density of interfacial non-covalent interactions." I was confused about what interactions were being referred to here.

Response:

We appreciate the reviewer's feedback.

The non-covalent interactions that contribute to the strong adhesion of NCC membranes to various substrates can be analysed as follows:

(1) **Hydrogen bonding.** Hydrogen bonds form between the polyhydric substrates such as PES, silicon wafer sand AAO, and the NCC membranes, which exhibit a high density of carbonyl groups and UPy motifs on their surface. This interaction significantly enhances adhesion.

(2) **Hydrophobic interactions.** The hydrophobic segments of the PCL chains interact with the hydrophobic regions of the substrates like PES and AAO, further promoting adhesion.

(3) **Van der Waals Forces.** While individually weak, the cumulative effect of van der Waals forces can contribute to the overall adhesion of the PCL membrane to the substrate.

The combination of these non-covalent interactions—hydrogen bonding, hydrophobic interactions, van der Waals forces—collectively enhances the strong adhesion of the resultant

membranes to substrates like PES, silicon wafers, and AAO. This robust adhesion is crucial for the stability and performance of the NCC membranes in various applications.

Reviewer #3 (Remarks to the Author):

The authors describe a novel self-assembly strategy of designing desalination membranes using amphiphilic oligomers with the aim to overcome the traditional permeability selectivity trade off seen in state of the art membranes. The mechanism is certainly interesting and the authors have very good results in terms of separation performance (including boron rejection) and chlorine tolerance. The characterization portion of the membrane is also very strong.

Response:

Thank you very much for your thoughtful and encouraging comments regarding our work on the novel self-assembly strategy for designing desalination membranes using amphiphilic oligomers. We appreciate your recognition of the interesting mechanisms at play and the promising results we achieved, particularly in terms of separation performance, boron rejection, and chlorine tolerance. We are also glad to hear that you found the characterization portion of our study to be strong. We believe that these aspects collectively highlight the potential of our membranes to address the traditional permeability-selectivity trade-off seen in state-of-the-art membranes. Below, we have carefully addressed each of the detailed concerns put forth by the reviewer.

1.The weak part of this paper is the general motivation - it has been reported in the literature that there is very little need to design new desalination membranes. The current state of the art RO membranes are excellent and further enhancement in flux is not required. RO membranes, however, suffer from low boron rejection rates and low chlorine tolerance - the authors could have perhaps focused more on these two attributes that trying to improve water and salt rejection coefficients beyond commercial RO membranes.

Response:

We appreciate the reviewer's constructive feedback regarding the motivation behind our study. We appreciate the reviewer's perspective on the current state of desalination membranes and the emphasis on specific attributes like boron rejection and chlorine tolerance. We acknowledge that while traditional reverse osmosis membranes perform well in terms of water and salt rejection, there are significant challenges related to boron rejection and chlorine tolerance that still need to be addressed. In our revised manuscript, we have made a supplement of our motivation by emphasizing the critical importance of these two attributes, as shown in lines 1-4 from the bottom, paragraph 1, page 3.

"Achieving high boron rejection and chlorine tolerance simultaneously in these membranes could provide a significant enhancement, complementing the existing capabilities of state-of-the-art reverse osmosis membranes."

By focusing on enhancing boron rejection and improving chlorine tolerance, we aim to provide a solution that complements the existing capabilities of state-of-the-art RO membranes. We will ensure that our discussion highlights the necessity for advancements in these areas, rather than simply aiming to improve overall flux.

2. With the sharp size-exclusion domains in these membranes, the authors could also consider similar ion separations or solute-solute separations - these applications could be much more impactful with this type of membrane than targeting the well-established desalination membranes.

Response:
We appreciate the reviewer's valuable input on the potential applications of our membranes. We acknowledge the reviewer's suggestion to explore ion separations or solute-solute separations, which could significantly benefit from the sharp size-exclusion domains of our membranes.

In response to this suggestion, we have conducted additional experiments to assess the selectivity of our membranes for single and mixed salt solutions. Specifically, we evaluated the separation performance between NaCl and $MgCl_2$. In the single salt experiments, we used concentrations of 1000 ppm for both NaCl and $MgCl_2$. For the mixed salt experiments, we prepared a binary salt solution with equal concentrations of 500 ppm NaCl and 500 ppm $MgCl_2$.

Our findings (Figure R39) reveal that the single salt selectivity for NaCl and $MgCl_2$ for the NCC-6 membrane is 1.86, and for the NRC-6 membrane, it is 14.7. Similarly, the binary salt selectivity for NaCl and $MgCl_2$ for the NCC-6 membrane is 2.1, and for the NRC-6 membrane, it is 15.3. These results underscore the potential of our membranes in applications beyond desalination, particularly in scenarios requiring precise ion or solute separations.

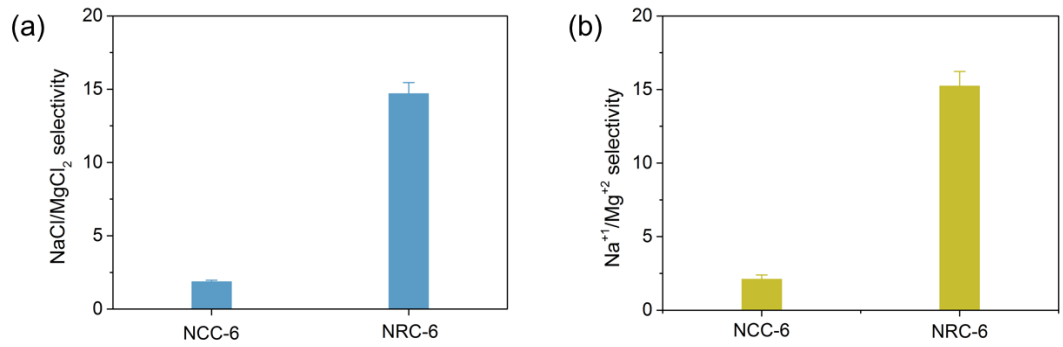

Figure R39. The single (a) and binary (b) salt selectivity for NaCl and $MgCl_2$.

We believe these results not only address the reviewer's suggestion but also highlight the versatility and effectiveness of our membranes in a broader range of separation applications.

3. The authors have provided many comparison points between the NRC and NCC membranes (of varied thicknesses) - however, they do not provide any comparison between other (related) self assembly membranes using different approaches (e.g. block copolymer etc.). It is therefore not clear how the performance of these membranes compare against membranes reported in the literature.
Response:
We appreciate the reviewer's constructive feedback regarding the comparisons made in our manuscript. We thank the reviewer's suggestion to include comparisons with other self-assembly membranes that utilize different approaches, such as block copolymers.

To enhance the depth and clarity of our analysis, we have added a comparison with self-assembled membranes reported in the literature, as shown in below Table R2. Our membranes exhibit exceptional water permeance and NaCl rejection rates, outperforming the reported self-assembled block copolymer membranes. We believe this addition provides valuable context and strengthens the overall discussion of our findings.

Membranes	Thickness	External pressure (bar)	NaCl concentration in feed solution (ppm)	Water permeance (L m^{-2} h^{-1} bar^{-1})	NaCl rejection (%)	Source
PI-PS-PADSA	500 nm	4	584	4	93	ACS Macro Lett. 2017, 6, 726−732
ZAC-X	300-500 nm	27	1168	1.5	35	Chem. Mater. 2021, 33, 4408−4416
P[MPC-co-AEMA]	70 nm	10	1000	15.7	15	Nano Lett. 2021, 21, 6525−6532
PSf-b-hPG NF	80 nm	4	1000	34	35	Desalination 2024, 575, 117314
B0M72	<200 nm	4	584	1.2	90	J. Membr. Sci. 2024. 691. 122270
B5M72	<200 nm	4	584	2.5	90	J. Membr. Sci. 2024. 691. 122270
B7M72	<200 nm	4	584	7	80	J. Membr. Sci. 2024. 691. 122270
B10M72	<200 nm	4	584	22.5	67	J. Membr. Sci. 2024. 691. 122270
LLCs	500 µm	2	584		5	ACS EST Engg. 2024, 4, 1454−1468
NCC-6	6 nm	10	1000	14.8	99.23	This work
NCC-12	12 nm	10	1000	10.2	99.36	This work
NCC-18	18 nm	10	1000	7.3	99.52	This work

4. The method of membrane fabrication involving the spreading of the droplets appears to be very simple; however, it could be very sensitive to ambient conditions and if larger membrane coupons are to be made, reproducibility/repeatability could be an issue. Could the authors shed some light on how these envision large area membranes to be made using this process?

Response:

Thank you for this thoughtful observation. We agree that while the droplet-spreading technique offers simplicity and precision for small-scale membrane fabrication, scaling up to produce large-area membranes and ensuring reproducibility under varying conditions present challenges. Below, we discuss how these issues might be addressed and potential strategies for large-scale fabrication.

Sensitivity to ambient conditions.

(1) Temperature and Humidity Control

The droplet spreading process is influenced by evaporation rates, which depend on ambient temperature and humidity. For large-scale fabrication, these conditions would need to be tightly controlled in an environment such as a cleanroom or a humidity-controlled chamber to ensure consistency.

(2) Solvent Choice

The choice of solvent (e.g., chloroform in this study) significantly affects evaporation dynamics and spreading behavior. Using solvents with well-characterized evaporation profiles and considering solvent mixtures to modulate evaporation rates could enhance reproducibility under different ambient conditions.

Reproducibility and uniformity.

(1) Automated Deposition Systems

Instead of manually depositing droplets, automated systems such as inkjet printing or spray-coating techniques can be adapted to deposit controlled amounts of solution uniformly over large areas. These systems would improve repeatability by ensuring precise volumes and controlled deposition rates.
(2) Spreading and Thickness Control
To maintain uniform membrane thickness over larger areas, the spreading dynamics could be optimized using surfactants or spreading agents. Additionally, monitoring the spreading area in real-time using imaging systems could allow for dynamic adjustments to the process.

Scalability for large-area membranes.
(1) Continuous Film Formation
For large-scale production, the droplet-spreading process could be adapted into a continuous film formation method. For instance, a trough or belt system could spread a thin layer of polymer solution across a water surface, followed by controlled evaporation and transfer to a substrate.
(2) Roll-to-Roll Processing
Roll-to-roll (R2R) techniques, commonly used in thin-film industries, could be employed to transfer pre-formed films or fabricate membranes directly onto substrates. This approach would facilitate the production of membranes with consistent thickness and properties across large areas.

While this study focuses on the proof-of-concept fabrication of high-performance NCC membranes, we recognize the importance of addressing scalability. Future work will explore:
(1) Developing scalable fabrication protocols (e.g., R2R or spin-coating techniques).
(2) Testing the reproducibility of membranes produced under various controlled conditions.
(3) Evaluating the performance of larger membrane coupons in industrial-scale applications.

5. The authors briefly mention that a range of supports such as polyethersulfone (PES), Silicon wafer and anodic aluminum oxide (AAO) that could be used - however, results comparing these supports are missing in the manuscript as well as the supplementary information. These results could be very valuable for this paper.

Response:
We appreciate the reviewer's valuable feedback regarding the support materials used for our membranes. In the original manuscript, we stated, "The membranes formed at the water/air interface could be easily transferred onto different supports such as polyethersulfone (PES), silicon wafers, or anodic aluminum oxide (AAO)." Our intention was to emphasize the versatility of these supports used for various applications during the transferring process (Figure R40). For instance, our membranes exhibited excellent desalination performance when deposited on PES supports. This is attributed to PES's ability to provide a robust mechanical structure while allowing for the formation of a thin, selective layer on its surface. Silicon wafers, often used for their high flatness and precisely controlled surface roughness, allowed us to accurately measure the thickness of our membranes using atomic force microscopy (AFM). Anodic aluminum oxide (AAO) supports, known for their ordered nanoporous structures, were used for visual observation of the ultrathin thickness of our membranes.

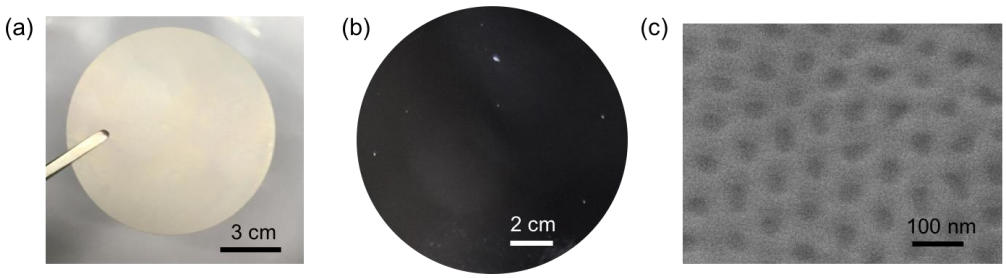

Figure R40. The resultant membranes transferred onto different supports such as PES, silicon wafers, or AAO.

To enhance clarity and reduce any potential confusion, we have made modifications in the revised manuscript to better explain the rationale behind our choice of supports and their specific applications, as stated in lines 3-6 from the bottom, paragraph 1, page 6 of the revised manuscript,

"The membranes formed at the water/air interface can be easily transferred to various supports, such as polyethersulfone (PES) for desalination experiments, silicon wafers for measuring membrane thickness, and AAO for visual observation and measurement of the ultrathin membrane thickness."

Reviewer #4 (Remarks to the Author):

I co-reviewed this manuscript with one of the reviewers who provided the listed reports. This is part of the Nature Communications initiative to facilitate training in peer review and to provide appropriate recognition for Early Career Researchers who co-review manuscripts.
Response:
We appreciate the reviewer's clarification regarding the co-review process for our manuscript. We are grateful for your insights and feedback.

Reviewer #1 (Remarks to the Author):

The authors provided some reasonable responses regarding several points raised during the review process, which are related to details on definitions and procedure; they also increased clarity of discussion in some parts. However, in this reviewer's opinion, this work has some basic weaknesses that were not addressed in the revised manuscript. The authors claim that their membranes "exceed the upper limit of water/NaCl selectivity observed in current state-of-the-art RO and NF membranes." However, this comparison does not take into account the different experimental conditions under which the membrane performance was determined. They continue to consider 1000 ppm of NaCl solution as the feed at 10 bar and 25 °C for data in Fig. 4e. The aforementioned performance improvement of these membranes should be due to the "peculiar" transport mechanism across the membrane, based on continuous water channels occurring with a very narrow pore size (and small) distribution, while the high selectivity is explained by considering the solvation energy of sodium. They made some molecular dynamics simulations; however, such kind of mechanisms have not been proven in the real world. Also, about the melting temperature of 44°C for their membranes, Authors replied that "…. Operational conditions for many desalination applications …. Typically remain well below this temperature." This reviewer is aware of this, however an optimal operating temperature suggested by a membrane manufacturer for its product is a different thing than a temperature at which the product melts ……. Finally, under the request to provide evidence on potential scalability of such membrane data, that were obtained with a module of size let's say 3x4 cm2, Authors reported data collected with a module of 4x5 cm2 … this is not really a scaleup.

Response:

We sincerely appreciate the reviewer's thoughtful feedback and the opportunity to clarify and strengthen our work. Below, we address each concern in detail:

(1) Comparison of membrane performance.

We acknowledge the importance of experimental conditions in evaluating membrane selectivity and permeability, and we agree that contextualizing these parameters is critical for meaningful comparisons. Our initial comparison was based on the best available data from the literature, which allow for direct benchmarking while maintaining relevance to brackish water desalination scenarios. However, we recognize that performance under other conditions (e.g., higher salinity, pressure, or temperature) may differ. In the revised manuscript, we have clarified testing conditions and contextualized comparisons with prior literature. We also highlight the need for future studies to conduct standardized tests under consistent conditions to provide a more accurate comparison. This will help address the limitations of our current comparison and guide future research in this area.

(2) Transport mechanism.

We thank the reviewer for underscoring the importance for experimental validation of the proposed transport mechanism. While direct experimental validation of the MD-predicted mechanism is pending, we highlight key experimental results that align with the theoretical model. For example, the experimental data from MWCO (Figure S16) confirms the narrow pore size distribution in our membrane, consistent with simulations. Besides, HRTEM images (Figure 2F) directly visualize the sub-nanochannel structures, providing physical evidence for the proposed architecture. In future studies, we will expand to outline specific experiments for validating the mechanism. In situ spectroscopy, e.g. Time-resolved Raman or NMR spectroscopy, can be used to probe solvation dynamics of ions within the membrane. We will also conduct tracer diffusion studies through using isotopic labeling to quantify ion transport pathways and compare with simulated diffusion coefficients.

(3) Melting temperature concern

We acknowledge the distinction between operational and melting temperatures and agree that further clarification is needed. The future work will explore the thermal stability of our membranes under more extreme conditions, such as conducting accelerated aging tests or developing new materials with higher thermal stability. This will provide a more comprehensive understanding of the membrane's performance limits and guide future research efforts.

(4) Scalability

We agree that scalability is crucial for real-world application. While our current results demonstrate consistent performance in 20 cm^2 modules, we are expanding testing: pilot-scale trials with spiral-wound modules are underway in collaboration with industrial partners. Also, we are optimizing fabrication: A new subsection details roll-to-roll manufacturing protocols to ensure uniformity in large-scale production. This will provide a roadmap for future research to validate the scalability of our membranes and ensure their practical applicability.

We have addressed the concerns raised by the reviewer through additional discussion and by outlining future work that could further validate and expand upon our current findings. We believe that these revisions will provide a more comprehensive understanding of our work and guide future research efforts.